Zero-Doppler Pseudorange Biases

J.-M. Sleewaegen, W. De Wilde, *Septentrio, Belgium*

Biographies

Jean-Marie Sleewaegen is system architect at Septentrio, Belgium, where he is responsible for GNSS signal processing, system design and technology development. Before joining Septentrio, he was with the Royal Observatory of Belgium to pursue his Ph.D. research. He holds a M.Sc. degree and a Ph.D. degree in electrical engineering from the Free University of Brussels. He received the ION Burka award in 1999.

Wim De Wilde joined Septentrio in 2002. As a system engineer he has been leading the architecture definition of most of the company's GNSS receiver hardware platforms and ASIC IP blocks. He holds a M.Sc. degree in electrical engineering from the University of Ghent.

Abstract

Accurate GNSS time transfer depends on the precise determination of pseudorange biases. The prominent source of pseudorange bias is the hardware delay in receiver elements (antenna, cable and receiver frontend), but other sources of bias do exist. This paper addresses a bias that has so far not received much attention in the GNSS community, and which specifically affects pseudoranges taken at small or zero Doppler. These biases are of particular relevance to time transfer based on geostationary satellites or to absolute receiver calibrations involving the simulation of geostationary satellites.

The paper starts by showing that GNSS pseudoranges can exhibit an oscillating error pattern when the Doppler is smaller than a few Hertz. At zero Doppler, some satellites are shown to be affected by a constant nanosecond-level bias. Examples from real-life datasets and GNSS simulations, and from different types of geodetic-grade receivers are given.

The paper describes the nature of this type of bias. It is explained why GNSS receivers tend to have difficulties producing accurate pseudoranges when the Doppler is lower than a few Hertz. It is shown that the resulting bias depends on the receiver digital sampling frequency and on the satellite PRN code and chipping rate. The size of the bias is quantified for the different GNSS constellations and signals and for typical sampling frequencies used in GNSS receivers employed for time transfer. It is shown that the GPS L1 C/A signals are the most affected, and that the effect is satellite-dependent, with some satellites showing biases of up to 30 cm (1ns).

It is then shown that the error can be predicted and compensated for when the relevant receiver parameters are known. The pseudorange errors from an uncorrected receiver and from a receiver applying a zero-Doppler bias compensation are compared, demonstrating the accuracy of the compensation.

Introduction

The starting point of the work presented in this paper is the observation that the pseudoranges from some GNSS satellites exhibit a glitch when the Doppler crosses zero. This is illustrated in Figure 1, which shows the noise on the L1 C/A pseudorange of GPS PRN#5 over a satellite pass above Leuven, Belgium. As expected, the noise increases at the beginning and end of the pass due to the lower elevation of the satellite. What is unexpected though is the glitch in the middle of the pass shortly after 12:00, which occurs exactly when the Doppler value crosses zero. Figure 2 is a close-up of the vicinity of the zero-Doppler point.
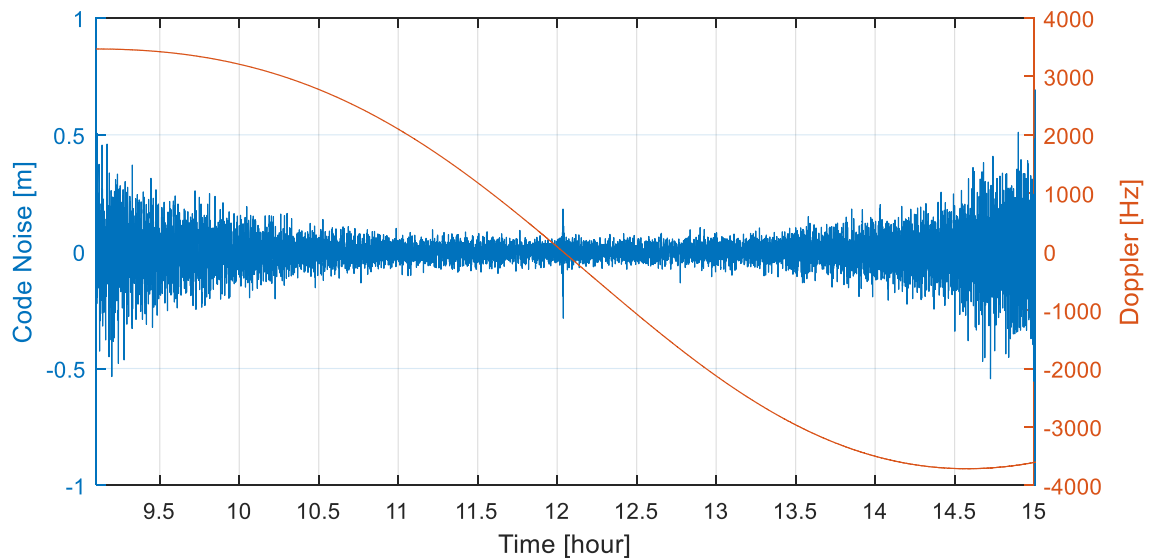
Figure 1 GPS L1 C/A pseudorange noise during a pass of PRN#5 (real-life signals, noise computed from the single difference between two receivers in zero-baseline configuration, and fed with the same frequency reference).
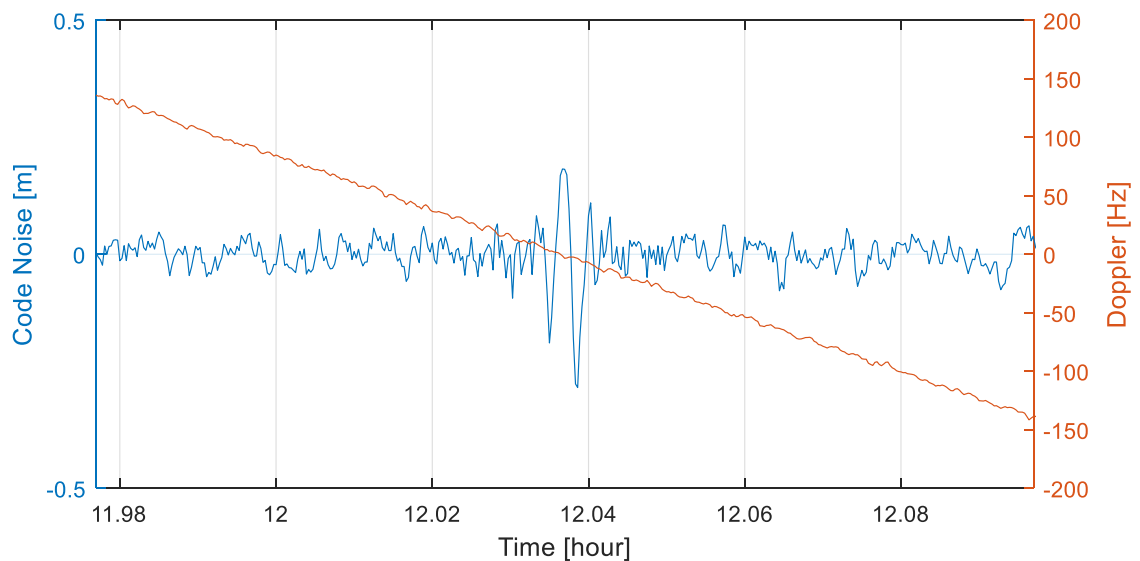

Figure 2 Close-up of the pseudorange noise at the zero-Doppler point of Figure 1.

The pseudorange is affected by a decimeter-level perturbation at the zero crossing of the Doppler. Further analysis reveals that this effect is satellite-dependent: some satellites exhibit such decimeter-level perturbation, others are almost unaffected.

In Figure 1, the noise was extracted from the single difference between pseudoranges from two Septentrio PolaRx5 receivers in zero baseline and tracking real-life GNSS signals. However, the phenomenon appears to affect other geodetic-grade receiver models as well, and is also visible in non-differenced pseudoranges. Figure 3 and Figure 4 show the pseudorange noise during a zero-Doppler crossing for geodetic-grade receivers from two other manufacturers (referred to as vendors A and B). These figures have been obtained from simulated GNSS signals with all error sources (atmospheric delays, multipath) turned off. The

noise is computed from the well-known code-minus-phase combination. In all cases, an oscillating error pattern can be seen around the Doppler zero-crossing, with a decimeter-level bias when the Doppler is zero.
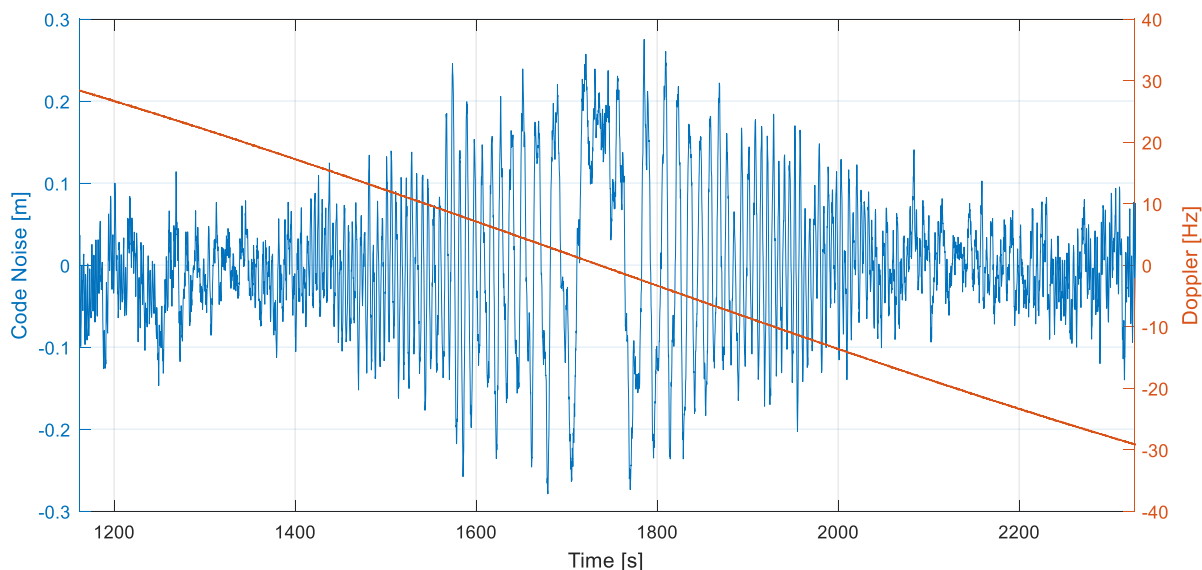

Figure 3 L1 C/A pseudorange noise near a zero-Doppler crossing for vendor A (simulated signal, noise computed from the code-minus-carrier combination).
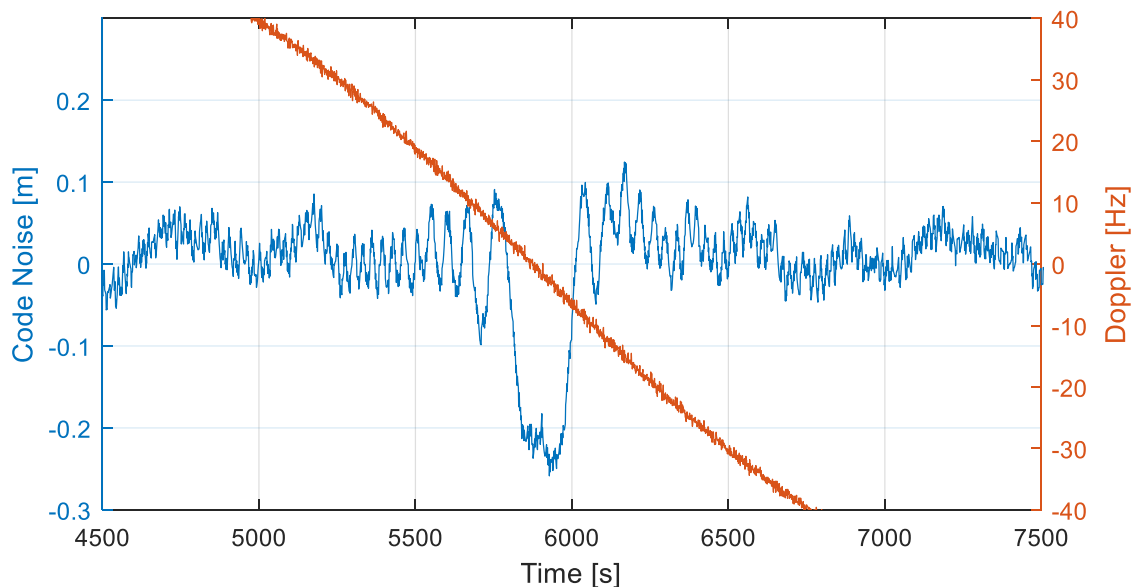

Figure 4 L1 C/A pseudorange noise near a zero-Doppler crossing for vendor B (simulated signal, noise computed from the code-minus-carrier combination).

These observations show that GNSS receivers have difficulties producing accurate pseudoranges during periods of small or zero Doppler. This phenomenon is known in low-end receivers [1][2], where the error can reach meters. It is less known though that geodetic-grade receivers are also affected. For GNSS satellites in MEO orbits, this error is not really a problem because it only affects a very short portion of the pass, as shown in Figure 1. However, this is not the case for geostationary satellites for which the Doppler can remain close to zero for a long time depending on the frequency offset of the receiver

clock. This problem is especially relevant to the timing community, where it is common practice to calibrate receiver hardware delays using simulated GNSS constellations involving constant zero-Doppler conditions [3][4][5].

In the following sections, we'll first explain the cause of the oscillating error pattern and of the bias at zero Doppler. We'll then quantify the bias for a particular receiver model best known to the authors (the Septentrio PolaRx5), and we'll show that the error can be accurately predicted and compensated for when the receiver parameters are known.

The origin of the Zero-Doppler Biases

GNSS satellites transmit ranging signals in the form of pseudorandom noise (PRN) codes, consisting of a succession of "+1" and "-1", the so-called "chips" of PRN codes. Figure 5 illustrates how such PRN code looks like when received by the receiver. This example shows 12 chips of a fictitious PRN code. The smooth transitions between the "+1" and the "-1" are the result of filtering of the RF signal by both satellite- and receiver-side circuitry.
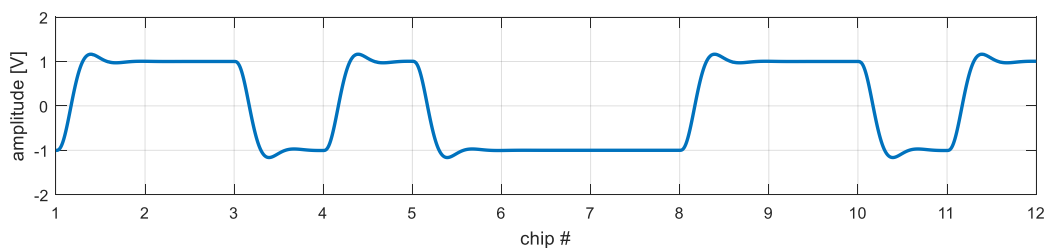

Figure 5 A snippet of a PRN code after downconversion in the receiver.

Pseudorange generation involves measuring the average position of the chip transitions of the PRN code received from a satellite. The averaging takes place in the receiver's delay-lock-loop (DLL) and is typically done over a time span of one second or longer depending on the DLL bandwidth.

The more chip transitions available per second, the more accurate pseudoranges can be determined, as the receiver can average over a larger number of transitions. This is the main reason why codes with high chipping rate, such as the GPS L5 codes with about 5000000 chip transitions per second, are more accurate than codes with low chipping rate, such as the GPS L1 C/A codes with "only" 500000 chip transitions per second.

All modern GNSS receivers process the signal in the digital domain, such that the DLL does not process the continuous signal shown in Figure 1, but discrete samples of it taken at a sampling frequency $F_{S,DLL}$ ($F_{S,DLL}$ is typically a few tens of MHz for geodetic-grade receivers). Note that $F_{S,DLL}$ is not necessarily equal to the sampling frequency at which the A/D conversion is done in the receiver. It is the frequency at which the samples are processed in the DLL section of the receiver.
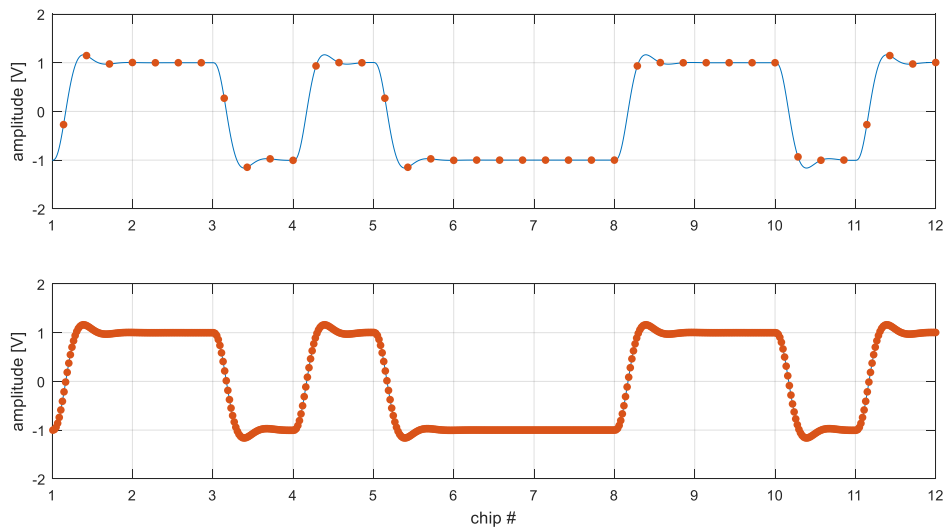
Figure 6 Illustration of the sampling process in a GNSS receiver. The upper panel shows a case of a relatively low sampling frequency (e.g. a few MHz). The lower panel illustrates a higher sampling frequency (e.g. a few tens of MHz).

Figure 6 illustrates the sampling process. The blue line is the analog signal and the discrete samples are marked by red dots. The upper panel shows the case of a receiver using a low value of $F_{S,DLL}$ while the lower panel corresponds to a receiver using a high value of $F_{S,DLL}$. For accurate determination of the position of the chip transitions, the DLL needs a sufficiently large number of samples falling in or close to the transitions, and these samples must be evenly distributed across the transitions. It is obvious that a receiver using a low DLL sampling clock will have greater difficulty producing accurate pseudoranges than a receiver using a high sampling clock as the chip transitions are more coarsely sampled.

The DLL sampling clock runs in the receiver time scale, and hence the discrete samples are taken at fixed intervals in the receiver time scale. The phase of the DLL sampling clock with respect to incoming PRN code depends on the range to the satellite (including all atmospheric delays and perturbations) and on the clock offset between the satellite and the receiver, i.e. it directly depends on the pseudorange to the satellite.

When the pseudorange varies with time, i.e. the Doppler is not zero, the phase of the DLL sampling clock with respect to the incoming PRN code changes continuously. Most GNSS PRN codes have a finite length and repeat every few milliseconds. Thanks to the pseudorange variation, the phase of the sampling clock will be different at each period of the PRN code. This is illustrated in Figure 7, which shows the position of the discrete samples for three successive periods of the PRN code when the pseudorange changes (red, orange and purple dots).
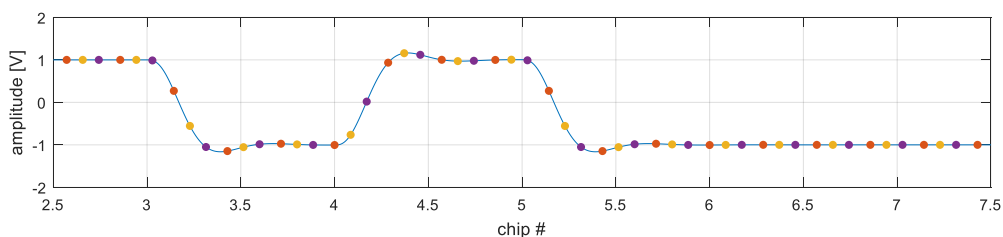

Figure 7 Phase of the discrete samples relative to the incoming PRN code. The red, orange and purple dots correspond to three different values of the pseudorange.

As can be seen in Figure 7, when the pseudorange changes, a given PRN transition is sampled at different points in the successive periods of the code. The pseudorange variation has the same effect as increasing the sampling rate. It introduces randomness in the phase at which the incoming PRN code is sampled, which means that the samples are, on average, better distributed across the chip transitions, at the benefit of the pseudorange accuracy.

This randomization effect disappears as the Doppler decreases towards zero. When the Doppler is precisely zero, the phase of the sampling clock stays constant with respect to the incoming PRN code. All periods of the PRN code are sampled exactly at the same phase. In that case, the discrete samples processed by the DLL exhibit a periodic pattern repeating indefinitely. Such a situation which does not change with time results in a bias. The bias will depend on the periodic sample pattern, which itself depends on the sampling rate and on the PRN code sequence, and hence on the satellite.

For a given satellite and given receiver parameters, the pseudorange bias is only a function of the phase of the incoming PRN code with respect to the DLL sampling clock, or more precisely, it is only a function of the pseudorange itself. This function is periodic because the same sample pattern repeats each time the pseudorange changes by one period of the DLL sampling clock multiplied by the speed of light ($c*T_{S,DLL}$ with $T_{S,DLL}=1/F_{S,DLL}$).

This is illustrated in Figure 8, which shows another example of Doppler zero-crossing error (in blue), together with the Doppler (upper panel), the pseudorange variation (middle panel) and the pseudorange modulo $c*T_{S,DLL}$ (lower panel). This figure has been obtained from simulated signals from a GNSS simulator where all other error sources were turned off. The pseudorange error (code noise) has been extracted using the code-minus-phase combination.
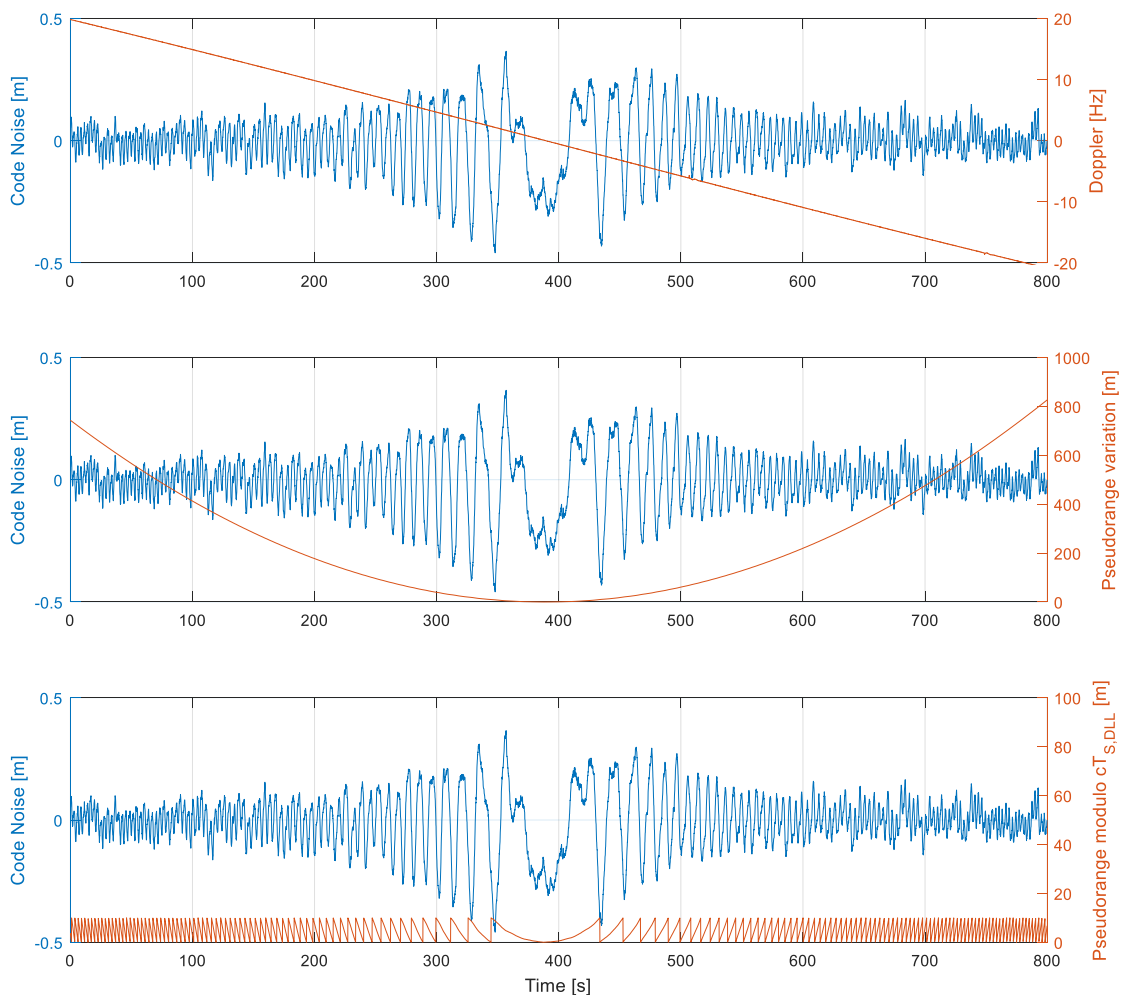

 Figure 8 Zero-Doppler pseudorange error (blue) and Doppler (upper panel), pseudorange variation (middle panel) and pseudorange modulo $c*T_{S,DLL}$ (lower panel).

The oscillating error pattern is a consequence of the fact that the pseudorange bias is a periodic function of the pseudorange itself. A single period corresponds to a change of pseudorange by $c*T_{S,DLL}$, as is clearly visible in the lower panel. The reason why the oscillations fade away when the Doppler increases is that they are filtered out by averaging in the DLL filter. When the Doppler exceeds about 15Hz, the error becomes negligible.

As a side note, two identical receivers connected to the same antenna and using the same frequency reference do not usually see equal pseudoranges, as their clock offset differ. As the bias depends on the pseudorange, it will therefore not be equal on the two receivers. This explains why the bias did not cancel out in the single difference shown in Figure 1.

Quantifying the Zero-Doppler Biases

The zero-Doppler pseudorange bias resulting from the discrete sampling of the incoming PRN code can be accurately predicted when the receiver parameters (essentially the DLL sampling frequency $F_{S,DLL}$) are known. The bias depends on the PRN code, and hence is different for each GNSS satellite. As explained in the previous section, it is a periodic function of the pseudorange, with a period of $c*T_{S,DLL}$.

We have used an accurate model of the sampling and DLL operation of the Septentrio PolaRx5 receiver to predict the zero-Doppler biases as a function of the pseudorange for that particular receiver. Figure 9 illustrates the result for L1 C/A pseudoranges from GPS PRN#1 and PRN#2.
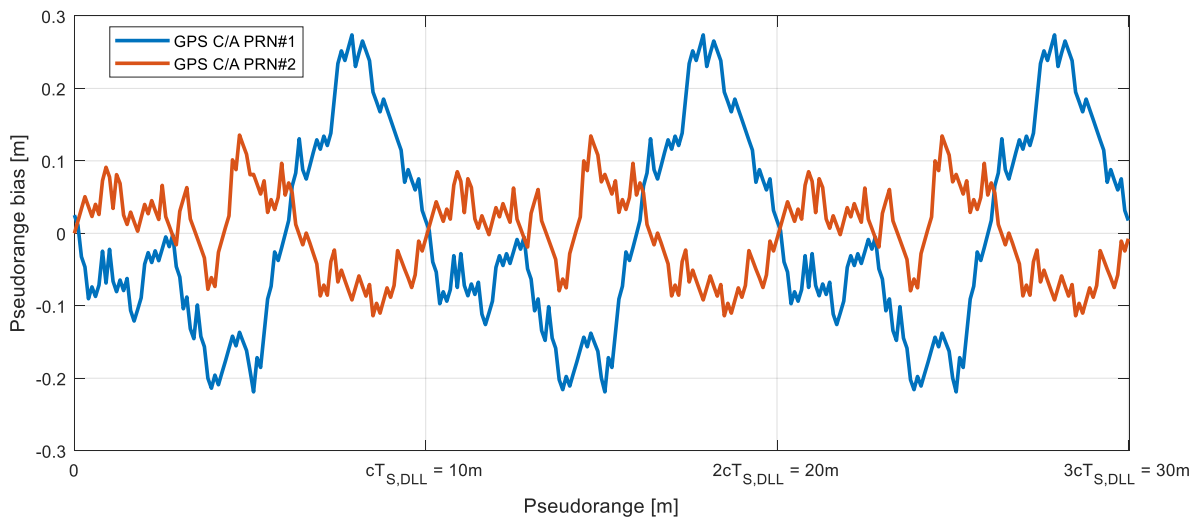

Figure 9 Zero-Doppler pseudorange bias for the L1 C/A code of GPS PRN#1 and #2 with the PolaRx5 receiver. The bias depends on the pseudorange with a period of $c*T_{S,DLL}$ = 10m.

In the PolaRx5, the DLL processes samples at a 30MHz rate ($F_{S,DLL}$=30MHz, $T_{S,DLL}$ = 33.33ns, $c*T_{S,DLL}$=10m). The figure shows the bias for a pseudorange varying from 0 to $3*c*T_{S,DLL}$ = 30m, and illustrates the $c*T_{S,DLL}$ (=10m) periodicity. The same pattern repeats indefinitely.

As can be seen in Figure 9, the bias is very different for PRN#1 and PRN#2, with the maximum bias being about 27cm for PRN#1 and 12cm for PRN#2. Other satellites would exhibit yet other bias patterns, each time with a different maximum value.

Figure 10 shows the maximum zero-Doppler bias for each GPS satellite and for two different signals (L1 C/A and L5Q). This figure indicates the maximum bias that can affect the L1 C/A and the L5Q pseudoranges in a PolaRx5 when the Doppler is zero.
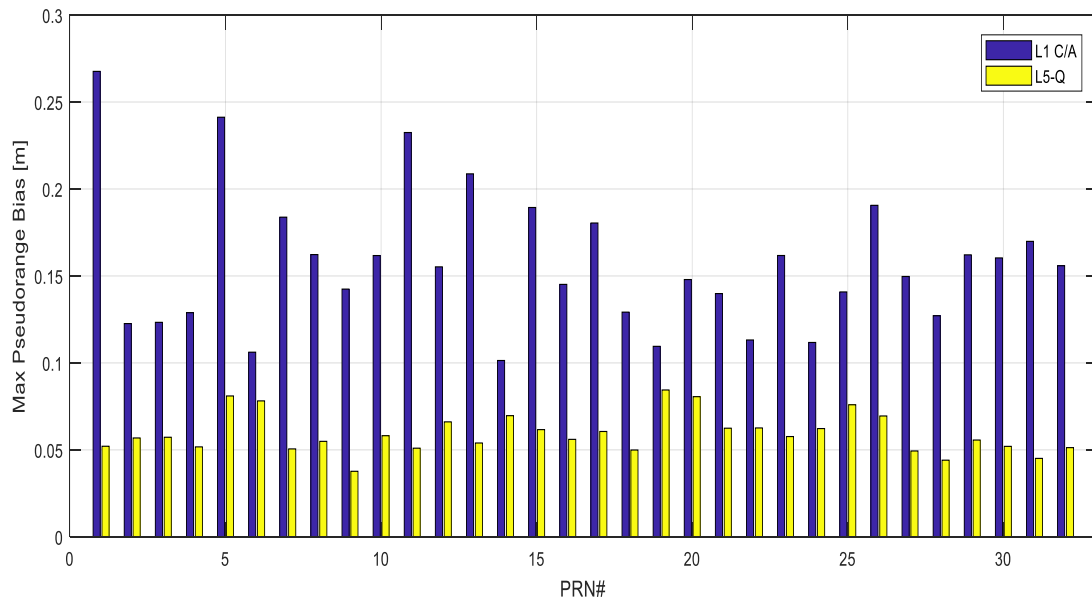
Figure 10 Maximum (worst case) PolaRx5 zero-Doppler bias for GPS C/A and L5Q pseudoranges as a function of the PRN number.

As can be seen in Figure 10, the largest maximum bias for the L1 C/A signal is for GPS PRN#1 (27cm), and the lowest maximum bias is for PRN#14 (10cm). The L5 signal performs significantly better than the L1 C/A signal, with the maximum bias being smaller than 10cm for all satellites. This is expected, as the L5 PRN codes are ten times longer than the L1 C/A PRN codes (1023000 chips vs 102300 chips). The maximum bias of the GPS L2CL pseudoranges is even smaller (millimeter level) due to the very long L2CL code. The bias is negligible for the GPS L2P pseudoranges as the P-code length is virtually infinite.
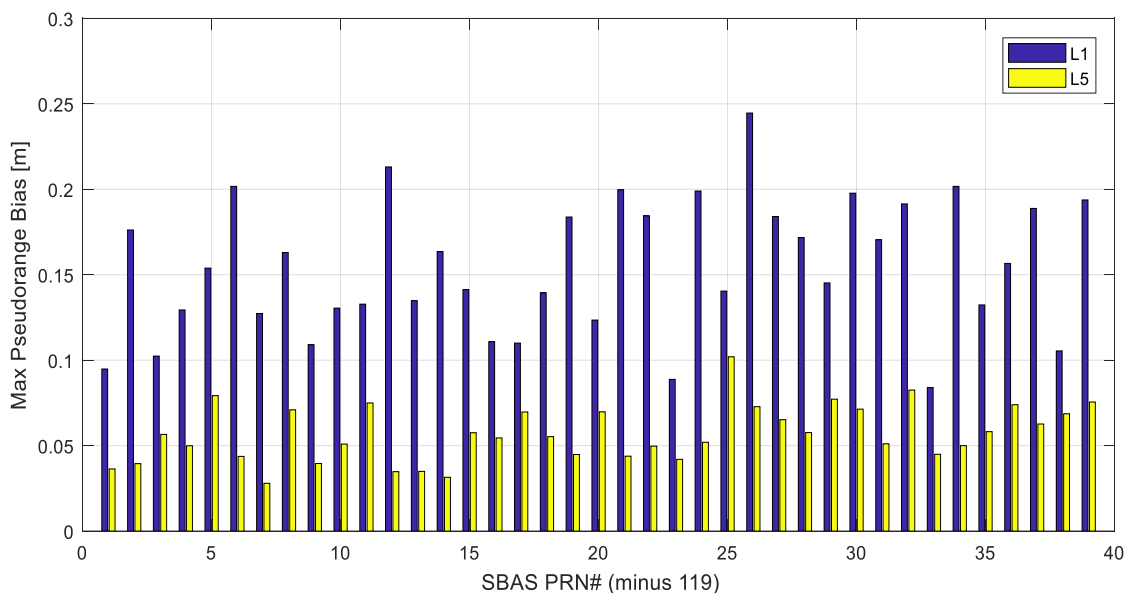

Figure 11 Maximum (worst case) PolaRx5 zero-Doppler bias for the SBAS L1 C/A and L5 pseudoranges.
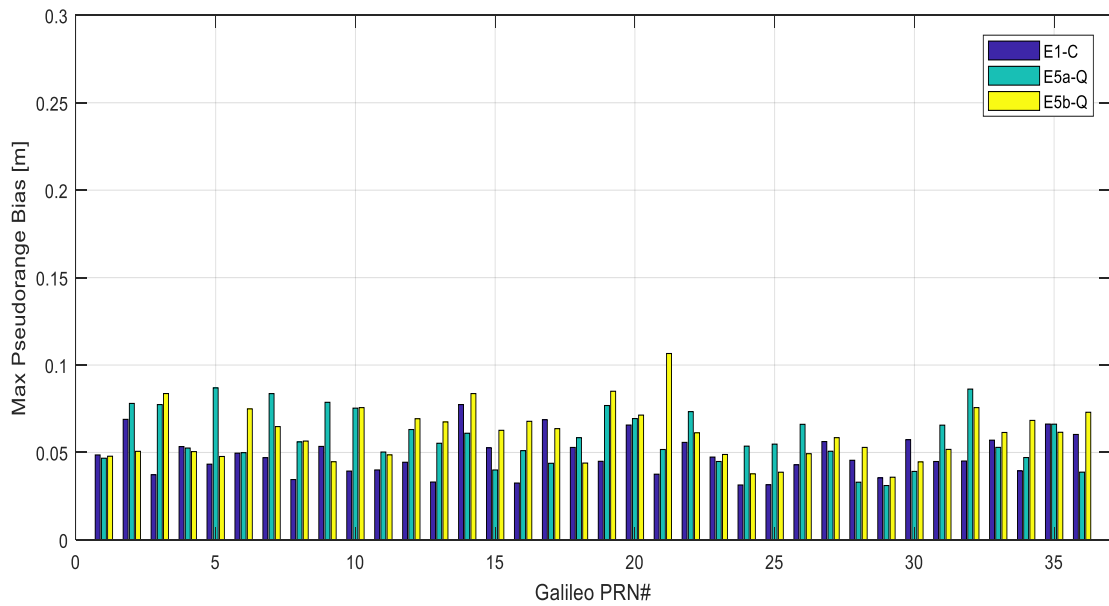
Figure 12 Maximum (worst case) PolaRx5 zero-Doppler bias for Galileo E1, E5a and E5b pseudoranges.
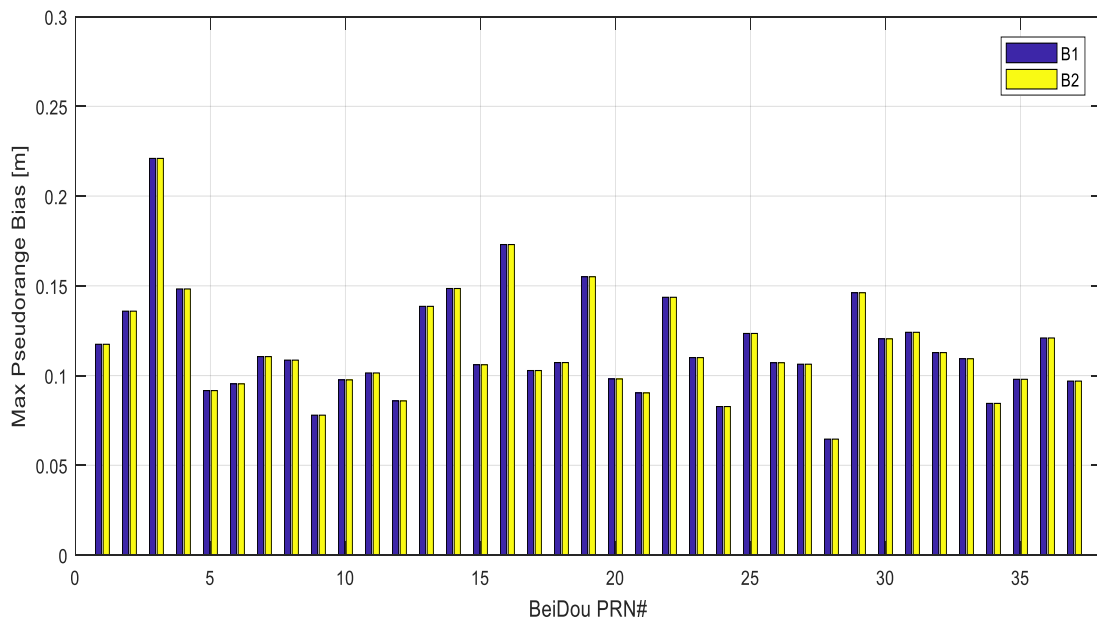

Figure 13 Maximum (worst case) PolaRx5 zero-Doppler bias for BeiDou B1 and B2 pseudoranges (the B1 and B2 codes are identical, and so are the biases).

Figure 11, Figure 12 and Figure 13 show the maximum bias for the SBAS, Galileo and BeiDou satellites respectively. As expected, the SBAS biases are in the same order of magnitude as the GPS biases, because SBAS and GPS L1 C/A and L5 signals rely on the same family of PRN codes. The biases of all Galileo E1, E5a, E5b codes are smaller than 10cm (except for E21), while BeiDou B1 and B2 biases fall in-between GPS and Galileo.

It is important to emphasize that the maximum error shown in the previous figures corresponds to a worst-case zero-Doppler bias. In fact, maximal biases occur only at specific values of the pseudorange (spaced by $c*T_{S,DLL}$ as explained earlier). In most cases, actual biases at zero Doppler will therefore be smaller. It should also be noted that the values in Figure 9 to Figure 13 depend on the receiver parameters, and are only applicable to Septentrio PolaRx5 receivers.

Compensation of Zero-Doppler Biases

When the receiver parameters are known, curves such as the ones shown in Figure 9 can be computed for all satellites and all signal types, as a function of the pseudorange. This means that the pseudorange error can be predicted and compensated for.

Figure 14 corresponds to Figure 8, but with the error prediction superimposed in red. It can be seen that the prediction accurately matches the actual error, which allows to compensate for it. The black trace in Figure 14 shows the pseudorange noise after applying the correction.
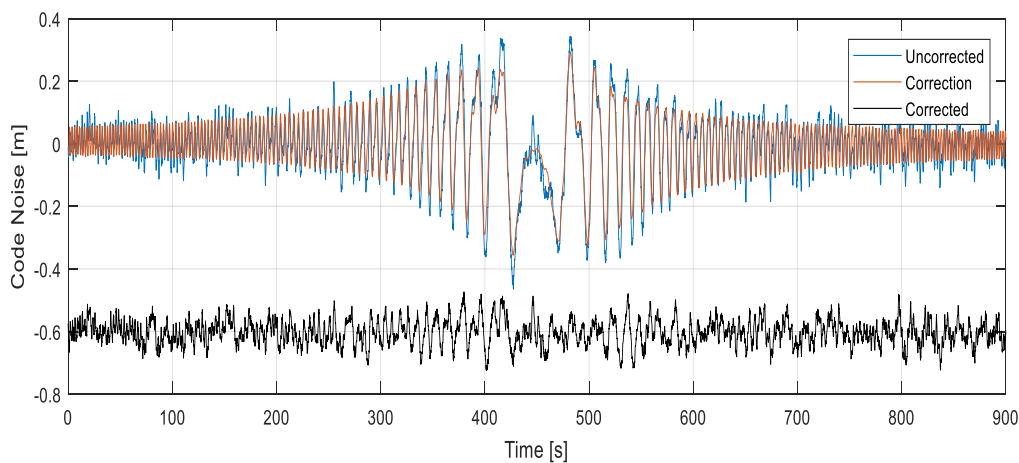

Figure 14 Pseudorange error (blue), its prediction (red), and the difference thereof (black).

This zero-Doppler error compensation can be applied in post-processing, but it requires knowing the internal parameters of the receiver. Such correction is preferably implemented in the receiver itself. We have done this in the firmware of the PolaRx5 receiver, and repeated the same zero-baseline test as the one shown in Figure 1. The code noise of GPS PRN#5 computed from single-differencing between two modified receivers is shown in Figure 15.

It can be seen that the glitch that was visible at the zero-crossing of the Doppler in Figure 1 disappeared with the modified firmware. In view of the results, future versions of the PolaRx5 firmware will incorporate this zero-Doppler bias compensation.
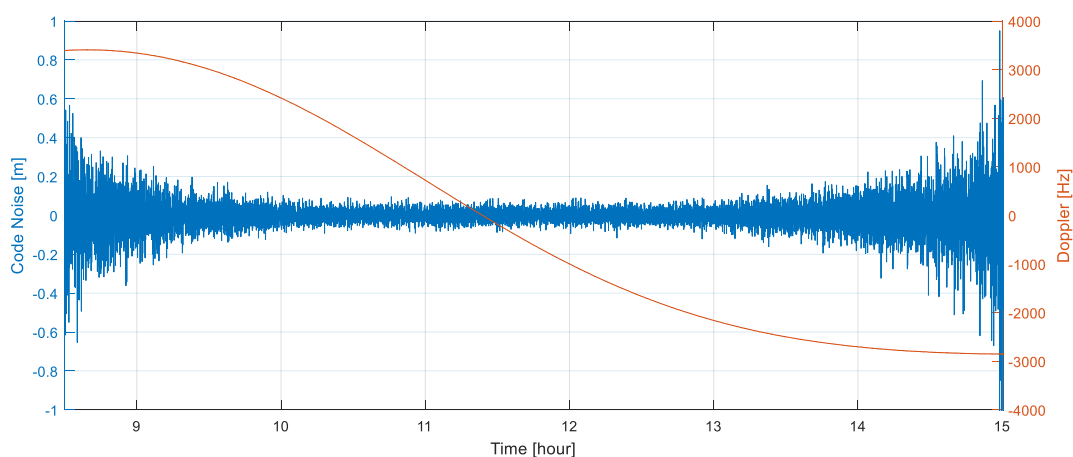
Figure 15 GPS L1 C/A pseudorange noise during a pass of PRN#5, computed from the single-difference between two PolaRx5 receivers in zero-baseline configuration, and fed with the same frequency reference. The firmware on the receivers was adapted to compensate for the zero-Doppler bias.

Conclusions

We have shown that the time discretization in GNSS receivers can cause decimeter-level pseudorange biases when the Doppler is zero, i.e. when the pseudorange is constant over time.

The biases depend on the PRN code and hence on the satellite and on the signal type. It has been shown that they are periodic functions of the pseudoranges. The biases have been computed for the Septentrio PolaRx5 receiver, for the GPS, SBAS, Galileo and BeiDou signals, and it has been shown that the GPS C/A codes are the most affected, with biases reaching up to 27cm in the worst case.

During a typical GNSS MEO satellite pass, the zero-Doppler biases are observed only during short time intervals. Therefore, the impact is generally limited when processing a full pass. However, the biases are more significant for geostationary satellites. It is particularly a concern when doing an absolute calibration using a GNSS simulator with some satellites simulated as geostationary. In these cases, zero-Doppler biases cannot be neglected when interpreting the results.

It has been shown that the biases can be accurately predicted if the receiver parameters are known, which allows to apply a correction in the receiver firmware. This was implemented in the PolaRx5 receiver and proved to eliminate the biases.

Bibliography

[1] Akos, Dennis M., Pini, Marco, "Effect of Sampling Frequency on GNSS Receiver Performance", *NAVIGATION, Journal of The Institute of Navigation*, Vol. 53, No. 2, Summer 2006, pp. 85-96

[2] Tran, V. T., Shivaramaiah, N. C., Nguyen, T. D., Dempster, A. G., "The effect of sampling frequency and front-end bandwidth on the DLL code tracking performance", *Proceedings of the IGNSS Symposium 2015*

[3] Plumb, J., Larson, K M., White, J., Powers, E.," Absolute Calibration of a Geodetic Time Transfer System", *IEEE Transactions on Ultrasonics, Ferroelectrics, and Frequency Control*, Vol. 52, Issue: 11, Nov. 2005

[4] Grunert, U., Thoelert, S., Denks, H., Furthner, J., "Absolute Calibration of Time Receivers with GPS/Galileo HW Simulator", *22nd European Frequency and Time Forum (EFTF08)*

[5] B. P. B. Elwischger, M. Suess, S. Thoelert,J. Furthner, "Absolute calibration of dual frequency timing receivers for Galileo", *The European Navigation Conference, April 2013 (ENC 2013)*